

Effects induced by a 50 Hz electromagnetic field and doxorubicin on Walker-256 carcinosarcoma growth and hepatic redox state in rats

Valerii E. Orel, Mykhailo Krotevych, Olga Dasyukevich, Oleksandr Rykhalskyi, Liubov Syvak, Helena Tsvir, Dmytro Tsvir, Lyudmyla Garmanchuk, Valerii B. Orel, Iryna Sheina, Vladyslava Rybka, Nataliia V. Shults, Yuichiro J. Suzuki & Sergiy G. Gychka

To cite this article: Valerii E. Orel, Mykhailo Krotevych, Olga Dasyukevich, Oleksandr Rykhalskyi, Liubov Syvak, Helena Tsvir, Dmytro Tsvir, Lyudmyla Garmanchuk, Valerii B. Orel, Iryna Sheina, Vladyslava Rybka, Nataliia V. Shults, Yuichiro J. Suzuki & Sergiy G. Gychka (2021) Effects induced by a 50 Hz electromagnetic field and doxorubicin on Walker-256 carcinosarcoma growth and hepatic redox state in rats, *Electromagnetic Biology and Medicine*, 40:4, 475-487, DOI: [10.1080/15368378.2021.1958342](https://doi.org/10.1080/15368378.2021.1958342)

To link to this article: <https://doi.org/10.1080/15368378.2021.1958342>



© 2021 The Author(s). Published with license by Taylor & Francis Group, LLC.



Published online: 16 Aug 2021.



[Submit your article to this journal](#)



Article views: 2364



[View related articles](#)



[View Crossmark data](#)



Citing articles: 2 [View citing articles](#)

Effects induced by a 50 Hz electromagnetic field and doxorubicin on Walker-256 carcinosarcoma growth and hepatic redox state in rats

Valerii E. Orel ^{a,b}, Mykhailo Krotevych ^c, Olga Dasyukevich^a, Oleksandr Rykhalskyi ^a, Liubov Syvak^d, Helena Tsvir^e, Dmytro Tsvir^f, Lyudmyla Garmanchuk ^g, Valerii B. Orel ^{b,h}, Iryna Sheina ⁱ, Vladyslava Rybka ^j, Nataliia V. Shults ^j, Yuichiro J. Suzuki ^j, and Sergiy G. Gychka^k

^aMedical Physics and Bioengineering Research Laboratory, National Cancer Institute, Kyiv, Ukraine; ^bBiomedical Engineering Department, NTUU “Igor Sikorsky KPI”, Kyiv, Ukraine; ^cResearch Department of the Pathological Anatomy, National Cancer Institute, Kyiv, Ukraine; ^dResearch Department of Chemotherapy Solid Tumors, National Cancer Institute, Kyiv, Ukraine; ^eIndependent Researcher, Kyiv, Ukraine; ^fMedical Faculty, Bogomolets National Medical University, Kyiv, Ukraine; ^gDepartment of Biomedicine, NSC “Institute of Biology and Medicine” of the Taras Shevchenko National University of Kyiv, Kyiv, Ukraine; ^hResearch Department of Radiodiagnosics, National Cancer Institute, Kyiv, Ukraine; ⁱDepartment of Medical Physics and Biomedical Nanotechnologies, V. N. Karazin Kharkiv National University, Kharkiv, Ukraine; ^jDepartment of Pharmacology and Physiology, Georgetown University Medical Center, Washington, DC, USA; ^kDepartment of Pathological Anatomy 2, Bogomolets National Medical University, Kyiv, Ukraine

ABSTRACT

We compare the effects of an extremely low-frequency electromagnetic field (EMF) with the chemotherapeutic agent doxorubicin (DOX) on tumor growth and the hepatic redox state in Walker-256 carcinosarcoma-bearing rats. Animals were divided into five groups with one control (no tumor) and four tumor-bearing groups: no treatment, DOX, DOX combined with EMF and EMF. While DOX and DOX + EMF provided greater inhibition of tumor growth, treatment with EMF alone resulted in some level of antitumor effect ($p < .05$). Superoxide dismutase, catalase activity and glutathione content were significantly decreased in the liver of tumor-bearing animals as compared with the control group ($p < .05$). The decreases in antioxidant defenses accompanied histological findings of suspected liver damage. However, hepatic levels of thiobarbituric acid reactive substances, an indicator of lipid peroxidation, were three times lower in EMF and DOX + EMF groups than in no treatment and DOX ($p < .05$). EMF and DOX + EMF showed significantly lower activity of serum ALT than DOX alone ($p < .05$). These results indicate that EMF treatment can inhibit tumor growth, causing less pronounced oxidative stress damage to the liver. Therefore, EMF can be used as a therapeutic strategy to influence the hepatic redox state and combat cancer with reduced side-effects.

ARTICLE HISTORY

Received 27 April 2021
Accepted 26 June 2021

KEYWORDS

Electromagnetic field; doxorubicin; Walker-256 carcinosarcoma; oxidative stress; hepatic redox state

Introduction

Cancer has been the second leading cause of death for over a century, reaching 18 million new cases worldwide in 2018. World Health Organization (WHO) predicts at least a 70% increase in the number of cancer-related deaths by 2030 (Copur 2019; Ferlay et al. 2019). Current cancer treatments, including tumor surgery, chemotherapy, immunotherapy and hormonal therapy, have some inherent limitations and side effects (Bernini and Bencini 2012; Haanen et al. 2017).

Non-ionizing electromagnetic fields (EMF) have been shown to exert antitumor effects *in vitro* and *in vivo* (Muramatsu et al. 2017; Omote et al. 1990). Clinical trials focused on the antitumor efficacy of EMF given as the primary or adjunctive therapy may contribute additional support for treatment outcomes and patient

survival. One potential advantage of EMF is that magnetic fields cause less damage to normal tissues than other cancer treatments (Tatarov et al. 2011). The tissues, however, are vulnerable to chemotherapy toxicity and the energy of electric fields, commonly used in hyperthermia treatment (Glazer and Curley 2011). Previously most studies have only considered thermal effects of EMF on tumor cell killing, further investigations recognize the importance and advantages of non-thermal effects (Bystrom and Rivella 2015; Klimanov et al. 2018; Mattsson and Simko 2019; Wust et al. 2010; Xu et al. 2021). The application of magnetic fields ranging between 0.3–0.4 T increased the oxidation rate of a hydrocarbon by 10–70% with a markedly accelerated initiation phase and reduced chain termination. The biological effects of EMF are associated with the triplet-

CONTACT Valerii E. Orel  valeriiorel@gmail.com  Head of Medical Physics and Bioengineering Research Laboratory, National Cancer Institute, 33/43 Lomonosov Str, Kyiv 03022, Ukraine

This article has been corrected with minor changes. These changes do not impact the academic content of the article

© 2021 The Author(s). Published with license by Taylor & Francis Group, LLC.

This is an Open Access article distributed under the terms of the Creative Commons Attribution-NonCommercial-NoDerivatives License (<http://creativecommons.org/licenses/by-nc-nd/4.0/>), which permits non-commercial re-use, distribution, and reproduction in any medium, provided the original work is properly cited, and is not altered, transformed, or built upon in any way.

singlet spin transitions in free radical pairs. Spin-dependent electron transport can be useful for elucidating the oxidation mechanism of organic compounds, e.g., lipids and proteins (Pliss et al. 2017). The mechanism underlying the antitumor activity of EMF is based on the increased generation of reactive oxygen species (ROS) and change in antioxidant systems.

The current understanding of redox state in tumor development involves a complex interplay between prooxidants and antioxidants (Hawk et al. 2016). Despite the essential role of oxygen in cellular respiration, natural metabolism is not limited to ROS but also gives rise to reactive nitrogen species. Exposure to endogenous and exogenous oxidants, such as hydroxyl radical ($\bullet\text{OH}$), hydrogen peroxide (H_2O_2) and superoxide radical ($\text{O}_2^{\bullet-}$), is an inevitable feature of living organisms. Hence, maintaining redox homeostasis and protecting against oxidative stress is vital for cells. Superoxide dismutase, catalase and peroxidases are the main antioxidant enzymes that eliminate superoxides and peroxides. Some enzymes as methionine sulfoxide reductases and disulfide reductases/isomerases react to repair cellular damage. Antioxidants with low molecular weight, e.g., ascorbic acid, thiols, tocopherols, carotenoids, bilirubin and urate, serve as electron donors to prevent the oxidation of lipids, proteins, DNA and carbohydrates (Davies 2016).

Doxorubicin (DOX) is among the most widely prescribed anthracyclines to treat solid and hematologic tumors (Gastwirt and Roschewski 2018; Naruphontjirakul and Viravaidya-Pasuwat 2019; Upshaw et al. 2019; Yamashita et al. 2019). In addition to extensive hepatic metabolism leading to pronounced side effects, DOX dramatically alters the tumor redox state (Formelli et al. 1986). EMF acts on DOX-induced free radicals due to their paramagnetic properties. The influence of the magnetic and electric components of EMF converts the triplet state of lower electron energy to the excited singlet state in DOX-induced free radicals (Houston et al. 2016; Jin et al. 2012; Joshi et al. 2005; Usselman et al. 2014). The magneto-electric effects induce conformational changes in chemotherapeutic agents and, therefore, are critical for DOX intercalation into DNA (Nakata and Hopfinger 1980; Orel et al. 2019a). Tumor cells are more susceptible to damage from oxidative stress than normal cells. Electromagnetic modulation of oxidative stress is one approach to improve the antitumor efficacy of DOX, in which the generation of hydroxyl radicals under EMF causes DNA damage in the cells (Zorov et al. 2014). Moreover, the contribution of EMF to the redox state can be seen as a double-edged sword causing an

increased production or inhibition of ROS (Barnes and Greenebaum 2018; Orel et al. 2018).

The concept of redox modulation in cancer treatment can be employed as a combination of EMF and chemotherapy to reduce free-radical mediated toxicities. Nevertheless, the lack of fundamental understanding of ROS-mediated signaling pathways and the relationship between intra- and extracellular ROS interactions in the liver remains a major hurdle to developing anticancer treatments (Bauer 2014). The present study aims to compare the influence of DOX and EMF on the growth of Walker-256 carcinosarcoma and the hepatic redox state.

Materials and methods

Laboratory animals

Noninbred female rats with body weight 140 ± 3 g were obtained from the vivarium of the National Cancer Institute (Kyiv, Ukraine) following a 2-week quarantine. The animals were implanted in the right hind dorsum with Walker-256 carcinosarcoma cells (2×10^6 in 200 μl medium 199). The current study followed the design recommendations of (Shaw et al. 2017).

The rats were divided into one control (no-tumor) and four tumor-bearing groups ($n = 10$ per group): no treatment, DOX, DOX + EMF and EMF treatment. DOX was given intravenously 1.5 mg/kg of body weight in 0.3 mL saline on day 2 after tumor implantation. Animals received EMF in the prone position every other day 5 times in total. EMF treatment involved immobilization of anesthetized with 1–2% isoflurane rats in a horizontal volume coil for 80 min. Fiber-optic thermometers TM-4 (Radmir, Ukraine) were used to monitor the temperature rise on the surface and inside the tumor below 33 °C (Figure 1). Animal studies complied with the Law of Ukraine N 3447-IV regarding the protection of animals from cruelty and European Directive 2010/63/EU regarding the use of animals for scientific purposes (Guillen 2012).

Electromagnetic field apparatus and exposure

An EMF inductor with the dimensions of $130 \times 80 \times 15$ mm was fixed in a plastic box during treatment. The distribution of EMF on the surface of the apparatus is shown in Figure 2. EMF comprised the electric component with a maximum strength of 1994 V/m, whereas the magnetic component had a strength of 2040 A/m, frequency of 50 Hz, and output power of 19 W.

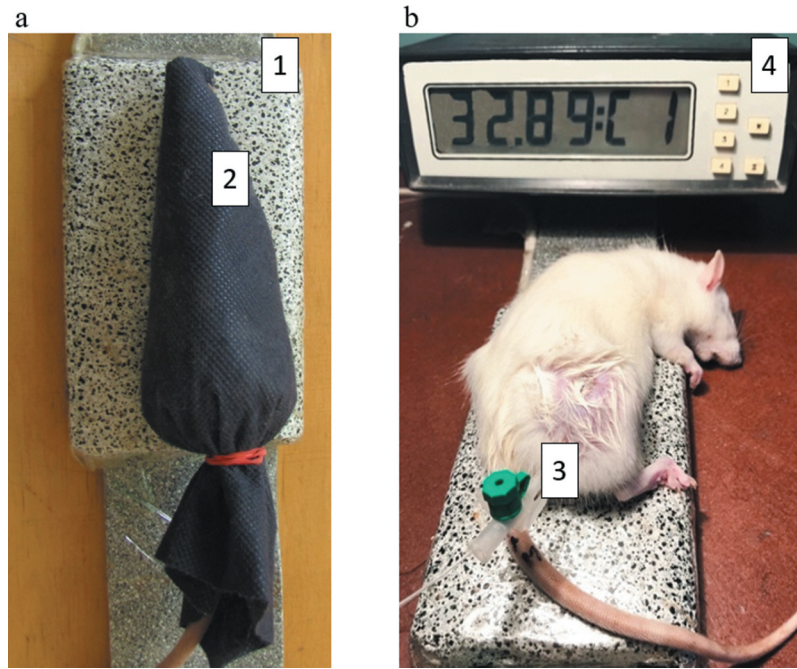


Figure 1. Animal positioning for extremely low-frequency electromagnetic irradiation (a): 1 – apparatus; 2 – rat position. Intratumoral temperature measurements (b): 3 – fiber-optic sensor, 4 – thermometer.

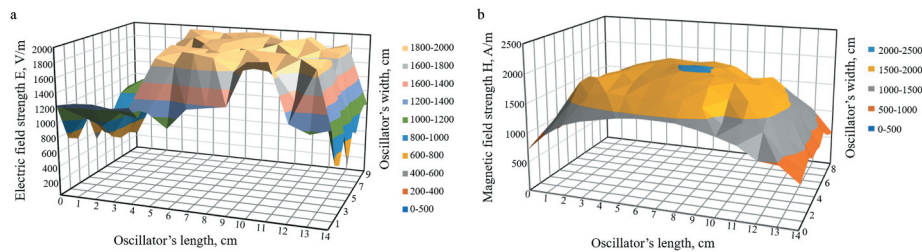


Figure 2. Distribution of electromagnetic fields on the apparatus surface: (a) electric field; (b) magnetic field.

Tumor growth and body weight

Tumor volumes were calculated from measurements of length (L), width (W) and height (H) taken three times each by an electronic digital caliper (Tayek et al. 1986). It was assumed that the tumors were approximately prolate spheroids with the volume (V):

$$V = L \cdot W \cdot D \cdot \pi/6 \quad (1)$$

Nonlinear kinetics of tumor growth was assessed through the growth factor ϕ by the autocatalytic equation:

$$dx/dt = \phi(x + x_0)(1 - x) \quad (2)$$

where Φ_0 and Φ_∞ respectively are the initial and the limiting tumor volumes; Φ is the tumor volume at the time t ; $x = (\Phi - \Phi_0)/(\Phi_\infty - \Phi_0)$ is the relative tumor

growth at the time t ; and $x_0 = \Phi_0/(\Phi_\infty - \Phi_0)$ is the relative tumor volume at the time $t = 0$ (Emanuel 1982; Orel et al. 2014).

Laboratory digital scales TBE-0.5–0.01a were used to measure body weight of tumor-bearing animals.

Histological evaluation

Tumor and liver tissue samples were collected from euthanized rats under sterile conditions and fixed for seven days in Bouin mixture, then embedded in paraffin, sliced into 5- μm sections and stained with hematoxylin-eosin-orange (H&E) (Kiernan 2008). H&E stained tissue slides were examined under a light microscope (Olympus BX-41, Olympus Europe GmbH, Japan) according to (Thoolen et al. 2010). The assessment of changes in

tumor and liver tissues was performed using the histological criteria defined by (Boroday and Chekhun 2018).

Texture analysis of digital pathology specimens quantified tumor heterogeneity based on standard deviation (SD) and brightness levels. The asymmetry plugin was applied to the liver images, which calculated the asymmetry parameter. CHAOS & IMAGE 1.0 software (developed by the National Cancer Institute of Ukraine, NCI) was used for computer-aided image analysis (Orel et al. 2007).

Assay of antioxidant parameters

The activity of superoxide dismutase (SOD), catalase (CAT), reduced glutathione (GSH) content, glutathione peroxidase (GP) and thiobarbituric acid reactive substances (TBARS) were used for assessing the hepatic redox state. Liver samples were washed and rapidly frozen at -70°C in phosphate buffered saline (PBS) with 1 mM ethylenediaminetetraacetic acid (EDTA) and 0.4 mM serine protease inhibitor (PMSF) at pH 7.0. Frozen samples were then thawed and gently homogenized in PBS with 1 mM EDTA and 0.4 mM PMSF, filtered and centrifuged at 10000 g for 15 min. Total protein was measured using a standard reagent kit (Diagnosticum Zrt, Hungary). Spectrophotometry characterized the levels of SOD, CAT, GSH, GP and TBARS.

The assay of SOD activity was based on the method described in (Salbitani et al. 2015). The ability of SOD to inhibit the tetrazolium dye reduction with superoxide, was measured by absorbance at 540 nm. For SOD, one unit was defined as the amount of enzyme providing 1% inhibition of tetrazolium dye reduction.

CAT activity was determined spectrophotometrically at 410 nm using a previously reported method with molybdenum salt (Goth 1991). The reaction started with the addition of 0.03% H_2O_2 solution. The activity was calculated based on the rate of H_2O_2 decomposition, where the extinction coefficient was $22.2 \text{ M}^{-1} \text{ cm}^{-1}$.

Colorimetric assay determined GSH content at 412 nm. GSH was oxidized by 5,5'-dithiobis-(2-nitrobenzoic acid) to glutathione disulfide and 5-thio-2-

nitrobenzoic acid (Tipple and Rogers 2012). GP activity was measured using unconsumed GSH after incubation with t-butyl hydroperoxide (Faraji et al. 1987).

TBARS were measured by absorbance at 532 nm. The extent of lipid peroxidation was expressed as TBARS given the extinction coefficient of $1.56 \times 10^5 \text{ M}^{-1} \text{ cm}^{-1}$ (Tukozkan et al. 2006).

Liver function tests

Blood samples were collected from the carotid artery immediately after euthanasia and centrifuged for 10 minutes at 1000 g. Measurements of alanine aminotransferase (ALT) and aspartate aminotransferase (AST) activity were completed by a standard analyzer (Diagnosticum Zrt, Hungary).

Statistical analysis

Experimental data were recorded and processed in Microsoft Excel (Microsoft Corporation, USA). Statistical tests were performed in STATISTICA 12.6 (StatSoft 2015).

Variables of tumor growth kinetics, liver antioxidant parameters, liver function tests and texture analysis were presented as the mean and the standard deviation of the mean (mean \pm SD). Data were tested for normality (Kolmogorov-Smirnov's test) and homogeneity of variance. A two-tailed Student's t-test determined the significance of differences between animal groups at the $p < .05$ level. Liver antioxidant parameters were compared between groups using one-way analysis of variance (ANOVA) followed by Tukey's HSD post-hoc test ($p < .05$). Kaplan–Meier survival analysis was performed and then compared with the log-rank test ($p < .05$).

Results

Tumor growth, body weight and survival

The results in Figures 3–5 show the tumor growth kinetics, body weight changes and survival of animals assigned to different study groups. Statistical analysis

Table 1. Walker-256 carcinosarcoma growth on day 15 after implantation (M \pm m).

Animal group	Tumor growth ϕ , day^{-1}
No treatment tumor	0.73 \pm 0.02
DOX	0.45 \pm 0.06 ¹
DOX + EMF	0.49 \pm 0.04 ¹
EMF	0.60 \pm 0.09 ¹²³

¹Statistically significant difference from no treatment tumor, $p < .05$;

²Statistically significant difference from DOX, $p < .05$;

³Statistically significant difference from DOX + EMF, $p < .05$.

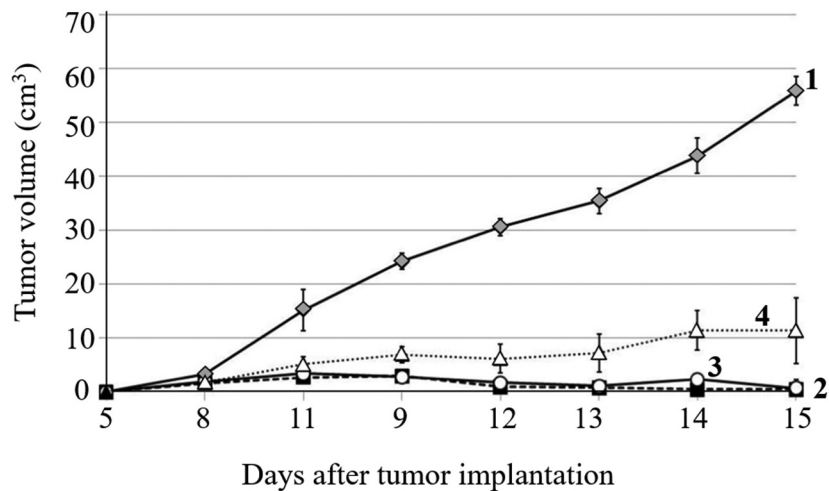


Figure 3. The growth kinetics of Walker-256 carcinosarcoma ($M \pm m$): 1 – no treatment; 2 – DOX; 3 – DOX + EMF; 4 – EMF.

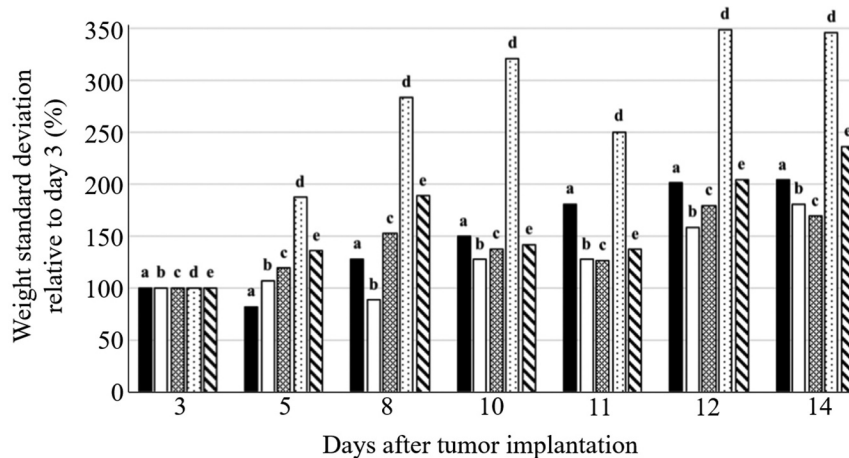


Figure 4. Changes in body weight of control and Walker-256 carcinosarcoma-bearing rats relative to day 3 after tumor implantation: a – control; b – no treatment tumor; c – DOX; d – DOX + EMF; e – EMF.

revealed significant differences between tumor-bearing rats receiving no treatment, DOX, DOX + EMF and EMF alone (Table 1). EMF treatment induced some level of antitumor effect, while its combination with DOX and DOX alone resulted in a greater Walker-256 carcinosarcoma growth inhibition (Figure 3).

Animals treated with DOX exhibited a reduced body weight gain as compared to DOX + EMF (144%) and EMF (26%), $p < .05$. The most pronounced relative changes in body weight were observed in DOX + EMF treatment (Figure 4), demonstrating the complex interactions between the combined treatment and the tumor-bearing host (Safdie et al. 2012). There were no significant differences in body weight changes between no-treatment and DOX groups during the early stage of tumor development (the first 8 days following implantation).

Survival rates of tumor-bearing animals were consistent with Walker-256 carcinosarcoma growth kinetics across the duration of the study. Each treatment resulted in increased survival as compared with the no-treatment group. DOX and DOX + EMF treatments led to the extended survival (100%) of tumor-bearing rats, while EMF alone resulted in 70% overall survival (Figure 5).

Histological findings

Histological changes in tumors obtained from Walker-256 carcinosarcoma-bearing animals are shown in Figure 6 and Table 2. In no-treatment group tumors had carcinomatous and sarcomatous components mostly with fibrotic tissue and interstitial edema (Figure 6a). However, numerous necrotic foci were present in animals treated with DOX. Tumors showed structural

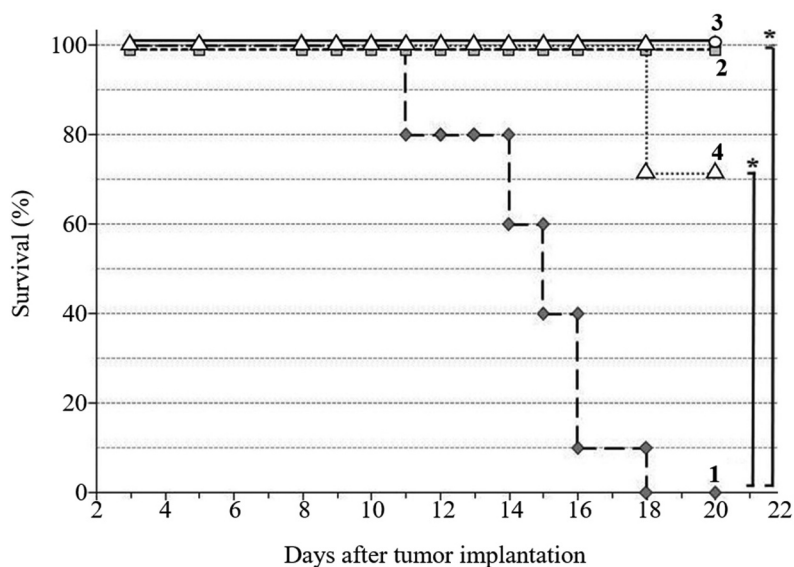


Figure 5. Overall survival of Walker-256 carcinosarcoma-bearing rats 20 days after tumor implantation: 1 – no treatment; 2 – DOX; 3 – DOX + EMF; 4 – EMF. * Statistically significant difference from no-treatment tumor, $p < .05$.

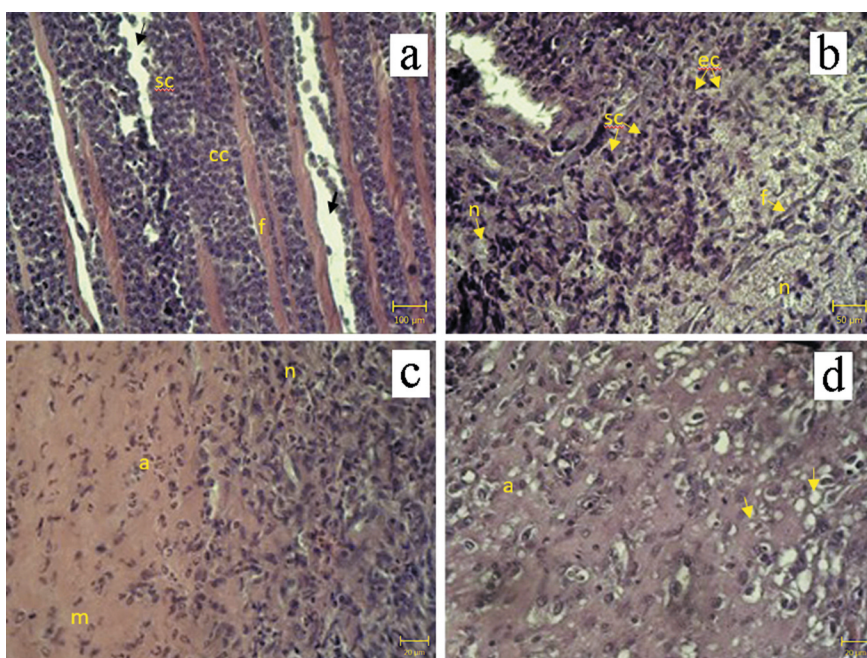


Figure 6. Histological findings in Walker-256 carcinosarcoma. H&E stain. (a) no-treatment group: sarcomatous (sc), carcinomatous (cc) components, fibrotic tissue (f) and interstitial edema (arrow), magnification x100; (b) DOX treatment: sarcomatous (sc), epithelioid (ec) components, fibrotic tissue (f) and necrosis of tumor cells (n), magnification x200; (c) DOX + EMF treatment: necrosis (n) and apoptosis (a) of tumor cells with extracellular matrix (m), magnification x400; (d) EMF: apoptosis of tumor cells (a) and pseudo-granular structures (arrows) magnification x400.

damage containing an epithelioid component and hyperchromic undifferentiated cells. Some tumors also underwent fibrotic changes within the extracellular matrix following DOX treatment (Figure 6b). After DOX + EMF treatment, animals demonstrated severe pleomorphism: many areas of necrosis, extracellular matrix

and at least minor foci of apoptosis (Figure 6c). EMF treated animals had apoptosis occurring with the development of pseudo-granular structures and fibrotic tissue. Although irradiated tumors were composed predominantly of the epithelioid component with eosinophilic content, they also showed small foci of central necrosis

Table 2. Tumor growth on 15th day after Walker-256 carcinosarcoma implantation ($M \pm m$).

Histological findings	Animal group			
	No treatment	DOX	DOX + EMF	EMF
Necrosis	+	+++	+++	++
Apoptosis	-	-	+	+++
Structural heterogeneity, arb. unit	40.7 \pm 2	36.6 \pm 1.8	24.0 \pm 1.2	22.6 \pm 1.1

The level of pronunciation: “-” not pronounced; “+” low pronounced; “++” moderate pronounced; “+++” high pronounced.

(Figure 6d) due to continued growth in the late phase (Casciato 2009; Schatten 1962). Texture analysis of tumor images revealed changes in structural heterogeneity after given treatments.

Figure 7 and Table 3 compare histological changes in the livers of Walker-256 carcinosarcoma-bearing animals. Liver tissue isolated from rats with implanted tumors receiving no treatment exhibited hepatocyte hypertrophy, ground glass changes and biliary hyperplasia (Figure 7a) because of host adaptation to the malignant process (Hargrove et al. 2017). DOX treatment alone resulted in swollen hepatocytes with empty nuclei, ground-glass changes in the cytoplasm, hypertrophy of surviving hepatocytes, biliary hyperplasia and neutrophil infiltration indicative of inflammatory response with mixed injury patterns (Figure 7b). Pathological changes observed in DOX + EMF group included less pronounced hepatic inflammation (Wieczorek et al. 2017) than in DOX group: ground-glass appearance, inflammatory cell infiltrates and bile duct hyperplasia

(Figure 7c). EMF treatment alone was associated with adaptive changes in the liver similar to those seen in the no-treatment group; however mild neutrophil infiltration was also present (Figure 7d). The asymmetry parameter computed in liver tissue images from no-treatment and DOX groups was higher than after DOX + EMF or EMF alone treatments.

Hepatic redox state and liver function tests

Analysis of the hepatic redox state revealed significant differences in antioxidant parameters between animal groups (Figure 8). TBARS levels showed potential hepatoprotective effects of EMF on lipid peroxidation as compared with DOX alone and no treatment. While the level of TBARS in animals receiving no treatment was about 8 times as much as in the control group (no tumor), DOX treatment resulted in 3 times as much as in EMF alone or DOX + EMF (Figure 8a). Enzymatic antioxidants in the liver, SOD and CAT, were also

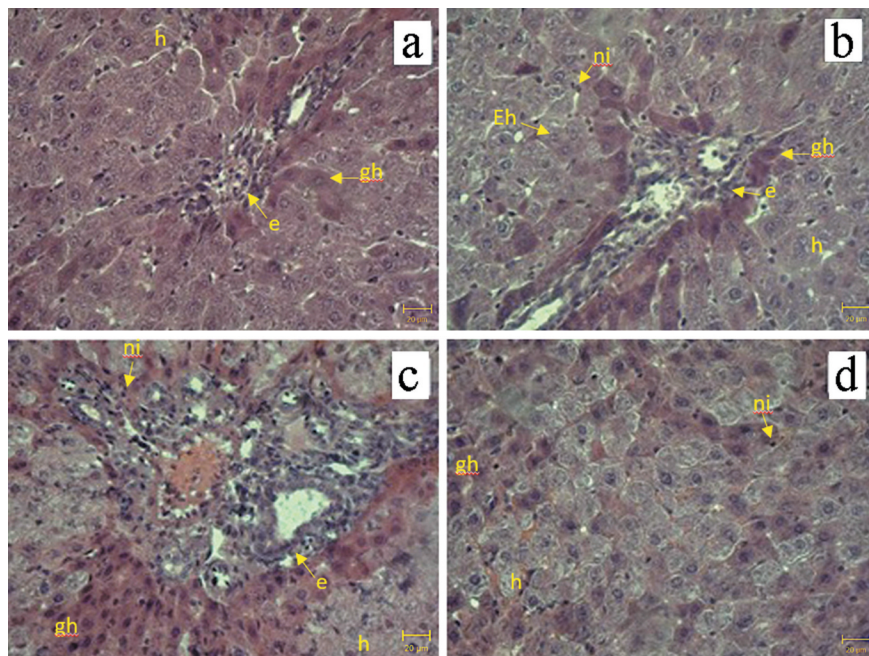


Figure 7. Histological findings in the liver of Walker-256 carcinosarcoma-bearing animals. H&E stain. (a) no treatment; (b) DOX; (c) DOX + EMF; (d) EMF: neutrophil infiltration (ni), hepatocytes with empty nuclei (Eh), hepatocyte hypertrophy (h), ground-glass hepatocytes (gh), biliary hyperplasia (e), magnification x400.

Table 3. Histological findings in the liver of Walker-256 carcinosarcoma-bearing rats.

Histological findings	Animal group			
	No treatment	DOX	DOX + EMF	EMF
Hepatocyte hypertrophy	++	++	++	+
Empty nuclei	-	+	-	-
Ground-glass hepatocytes	++	+	+++	+++
Biliary hyperplasia	++	+	+++	-
Neutrophil infiltration	-	++	+	+
Asymmetry parameter, arb. unit	0.58 ± 0.03	0.45 ± 0.02	0.18 ± 0.01	0.19 ± 0.01

The level of pronunciation: “-” not pronounced; “+” low or mild pronounced; “++” moderate pronounced; “+++” high pronounced.

affected by the tumor-host interactions and given treatment. SOD activity was about 5 times lower in the tumor-bearing groups than in the control. There was a significant difference in SOD activity between DOX + EMF treatment and DOX alone, $p < .05$ (Figure 8b). Similarly, the activity of CAT in the control group (no tumor) was 15 times as high as in tumor-bearing rats receiving no treatment. EMF + DOX and EMF alone resulted in significantly decreased CAT activity compared to DOX (Figure 8c). Besides a significant difference in GSH between the control and the tumor-bearing groups, only non-significant tendencies were apparent for decreased GSH content after EMF or DOX + EMF treatment compared to no treatment and DOX (Figure 8d). No significant differences were detected in GP activity between the groups.

Figure 9 shows the results of liver function tests in animal groups. Higher serum AST activity was found in tumor-bearing groups than in the control (no tumor). DOX, DOX + EMF or EMF treatments caused significantly higher AST activities than those observed in tumor-bearing animals receiving no treatment. Although the activity of ALT in the control group did not significantly differ from the no-treatment group, lower ALT activities were associated with EMF and DOX + EMF treatments ($p < .05$), suggesting a less pronounced form of liver damage (Kuzu et al. 2019).

Discussion

There is a growing body of evidence that EMF have a regulatory role in tumor development (Carpenter 2010; Kocaman et al. 2018; Tatarov et al. 2011) and anticancer

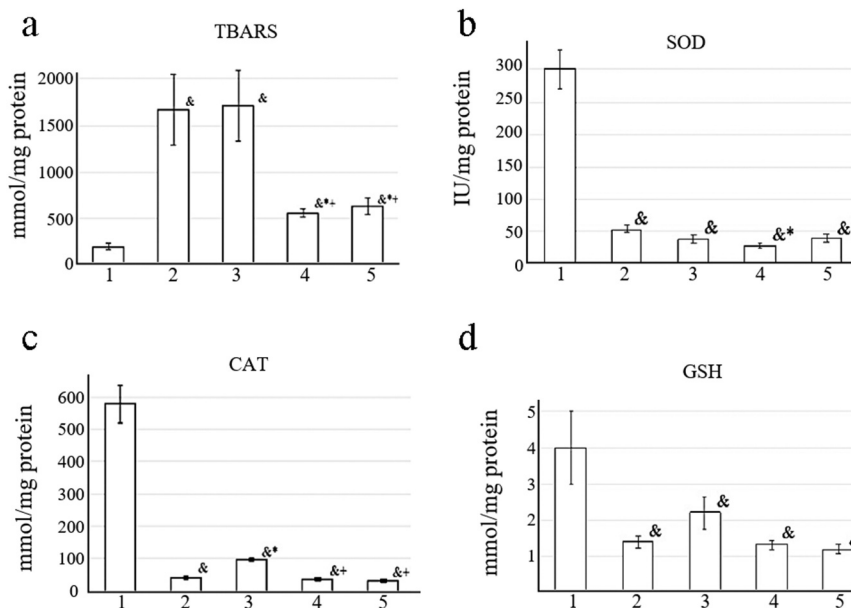


Figure 8. Hepatic antioxidant parameters: (a) TBARS, (b) SOD, (c) CAT, (d) GSH in 1 – control, 2 – no treatment, 3 – DOX, 4 – DOX + EMF, 5 – EMF groups.

&Statistically significant difference from control (no tumor), $p < .05$;

*Statistically significant difference from no-treatment, $p < .05$;

+Statistically significant difference from DOX, $p < .05$.

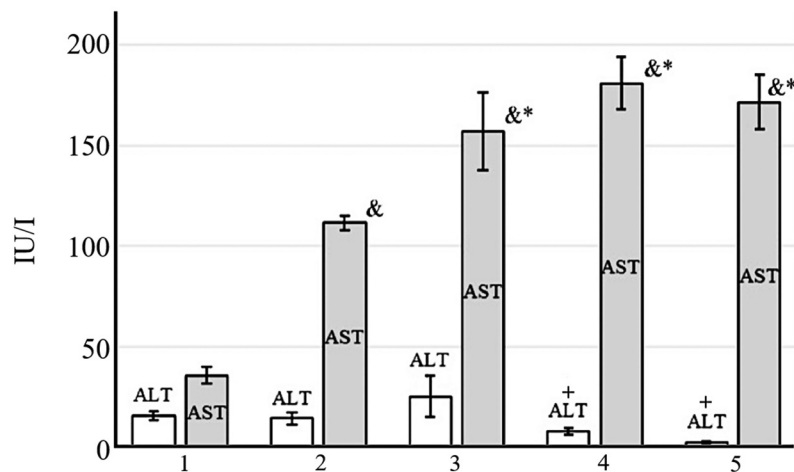


Figure 9. Serum alanine aminotransferase (ALT) and aspartate aminotransferase (AST) activities: control group with no tumor (1), Walker-256 carcinosarcoma-bearing animals receiving no treatment (2), DOX (3), DOX + EMF (4), EMF (5).

[&]Statistically significant difference from control without tumor, $p < .05$;

⁺Statistically significant difference from control no-treatment with the tumor, $p < .05$,

^{*}Statistically significant difference from tumor rats treated with conventional DOX, $p < .05$.

treatment (Cameron et al. 2014). One of the most difficult challenges related to the combined use of chemotherapeutic agents and EMF is to maintain efficacy and limit toxicities (Gewirtz et al. 2010; Thorn et al. 2011). Although DOX and DOX + EMF treatments resulted in enhanced antitumor effect than EMF alone, the present study emphasizes the potential application of EMF with less pronounced changes to the hepatic redox state in the Walker-256 animal model of breast cancer.

While tumor cells predominantly underwent necrosis in animals receiving DOX, morphological findings of apoptosis were observed after EMF alone. DOX + EMF treatment caused both necrosis and apoptosis of tumor cells. The development of fibrotic tissue accompanied tumor adaptation to DOX chemotherapy (Boroday and Chekhun 2018) and tissue replacement (Lushnikova et al. 2011). These results are consistent with previous investigations, which showed that the mechanism of tumor and liver cell death under the influence of EMF was apoptosis (Alves de Souza et al. 2017; Ghodbane et al. 2015; Lai 2019). The difference in texture features of tumor and liver tissue images between the groups was due to variability in DOX distribution within heterogeneous tumor vasculature and microenvironment, whereas the magnetic field could penetrate the tumor more evenly (Omote et al. 1990; Orel et al. 2017).

We focused on changes in liver tissue and oxidative stress as it is the main detoxifying organ in the human body. Hepatocytes undergo numerous metabolic processes to support redox homeostasis and biosynthetic

function. They are thus vulnerable to damage from oxidative stress. Mitochondria generate ROS as by-products of cellular respiration. Another source of ROS in the liver is microsomal enzymes involved in the metabolism of most chemotherapeutic agents (Sanchez-Valle et al. 2012). Liver macrophages (Kupffer cells) produce signaling molecules such as interleukins, tumor necrosis factor, and ROS to promote the immune response. Not only antigens but ROS products of lipid peroxidation can influence the activation of liver macrophages leading to inflammation (Cichoz-Lach and Michalak 2014). For this reason, the liver has antioxidant defense systems that maintain the redox state (Birben et al. 2012). Many patients, however, experience hepatotoxicity from treatment with chemotherapeutic agents and radiofrequency EMF (Ozgun et al. 2010; Videla 2009).

Tumor-bearing animals are more susceptible to lipid peroxidation and antioxidant enzyme downregulation (Deminice et al. 2016; Jumes et al. 2010). Measurements of antioxidant parameters found significant differences in the hepatic redox state between the control group (no tumor) and Walker-256 carcinosarcoma-bearing animals. SOD and CAT activities were significantly decreased in tumor-bearing animals compared to those with no-tumor. The activity of SOD after EMF significantly differed from DOX treatment; likewise, we reported lower CAT activity after EMF than DOX. Together, changes in antioxidant enzymes agree with earlier investigations that EMF alter antioxidant defense systems (Amara et al. 2009; Devrim et al. 2008;

Martínez-Sámano et al. 2010; Odaci et al. 2015). Higher GSH content observed in DOX-treated animals than in EMF or DOX + EMF treatment has been previously shown to facilitate tumor progression (Harris et al. 2015; Luo et al. 2018). Moreover, tumor-bearing animals showed histological features of more severe liver damage after DOX than EMF or DOX + EMF. The protective effect of EMF was based on inhibition of lipid peroxidation as determined by TBARS (Li et al. 2015). In addition to liver tissue examination, the activity of serum ALT was significantly lower in EMF and DOX + EMF than in DOX. Thus, our observations that a 50 Hz EMF alone or combined with DOX inhibit lipid peroxidation in the liver may be beneficial in the treatment of cancer patients.

Cysteine thiols in peptides and proteins are highly susceptible to oxidative stress. Oxidation of sulfhydryl groups forms disulfide bonds that mediate redox-regulated conformational switching of proteins. Glutaredoxins and thioredoxins are the enzymes to reduce oxidized thiols. The dynamic balance between reduced and oxidized thiol states is critical for gene transcription, cell signaling, antioxidant defense and apoptosis regulation. Further investigations should examine the effects of EMF and DOX-induced ROS (Simkó 2007; Topuz et al. 2017) on the thiol redox state under impaired regulation in cancer cells (Dirican et al. 2016).

One limitation of this study was that we only assessed the antitumor effects of EMF in the experimental animal model. The obtained results provide additional support for the combination DOX + EMF treatment with fewer side effects. Nonetheless, future research should consider the nonlinear relationship between given treatments and tumor-host interactions at different levels of biological organization, for example, antioxidant parameters, histological findings and tumor growth. The role of EMF to modulate ROS and antioxidants lacks a simple dichotomy; therefore, their interpretation requires a deep understanding of EMF effects on free radical pairs leading to redox, metabolic, genetic, epigenetic and morphological changes in the tumor and the host (Harris and DeNicola 2020; Orel et al. 2019b; Walton 2016).

Conclusion

In summary, this study indicates that a 50 Hz EMF treatment can inhibit Walker-256 carcinosarcoma growth and result in less pronounced oxidative stress damage to the liver of tumor-bearing rats. Although the combination treatment DOX + EMF and DOX alone showed a greater reduction of tumor growth, they also

caused more severe liver damage. The mechanism underlying hepatoprotective effects of EMF was based on inhibition of lipid peroxidation evident by TBARS. Serum ALT activity was significantly lower after EMF and its combination with DOX than DOX alone. Histological findings indicative of tumor cell apoptosis were observed after EMF treatment, whereas DOX led predominately to necrotic tumor cell death. These results provide additional support that non-ionizing EMF can be used to influence the hepatic redox state and combat cancer with reduced side effects.

Acknowledgments

The authors thank H. Kuznietsova, Ph.D., N. Dzubenko, Ph.D., A. Vorontsova, D.Sc. and V. Stegnii MSc. for providing excellent technical assistance for this study.

Disclosure statement

The authors declare no conflict of interest.

Funding

Funding: This research was funded by the Ministry of Health of Ukraine.

ORCID

Valerii E. Orel  <http://orcid.org/0000-0002-6319-4215>
 Mykhailo Krotevych  <http://orcid.org/0000-0002-5228-7491>
 Oleksandr Rykhalskyi  <http://orcid.org/0000-0001-6519-7316>
 Lyudmyla Garmanchuk  <http://orcid.org/0000-0002-5805-1930>
 Valerii B. Orel  <http://orcid.org/0000-0003-3653-0823>
 Iryna Sheina  <http://orcid.org/0000-0002-0293-4849>
 Vladyslava Rybka  <http://orcid.org/0000-0001-8828-6493>
 Nataliia V. Shults  <http://orcid.org/0000-0002-8643-3389>
 Yuichiro J. Suzuki  <http://orcid.org/0000-0001-6689-0497>

References

- Alves de Souza, C. E., H. M. Alves de Souza, M. C. Stipp, C. R. Corso, C. M. Galindo, C. R. Cardoso, R. L. Dittrich, E. A. de Souza Ramos, G. Klassen, R. M. Carlos, et al. 2017. Ruthenium complex exerts antineoplastic effects that are mediated by oxidative stress without inducing toxicity in Walker-256 tumor-bearing rats. *Free Radic. Biol. Med.* 110:228–39. doi:10.1016/j.freeradbiomed.
- Amara, S., T. Douki, C. Garel, A. Favier, M. Sakly, K. Rhouma, H. Abdelmelek. 2009. Effects of static magnetic field exposure on antioxidative enzymes activity and DNA in rat brain. *Gen. Physiol. Biophys.* 28:260–65. doi:10.4149/gpb_2009_03_260.

- Barnes, F., and B. Greenebaum. 2018. Role of radical pairs and feedback in weak radio frequency field effects on biological systems. *Environ. Res.* 163:165–70. doi:10.1016/j.envres.2018.01.038.
- Bauer, G. 2014. Targeting extracellular ROS signaling of tumor cells. *Anticancer Res.* 34:1467–82.
- Bernini, M., and L. Bencini. 2012. Multimodal treatment of gastric cancer: Surgery, chemotherapy, radiotherapy, and timing. *Int. J. Surg. Oncol.* (2012):246290. doi:10.1155/2012/246290.
- Birben, E., U. M. Sahiner, C. Sackesen, S. Erzurum, O. Kalayci. 2012. Oxidative stress and antioxidant defence. *World Allergy Organ. J.* 5:9–19. doi:10.1097/WOX.0b013e3182439613.
- Boroday, N. V., and V. F. Chekhun. 2018. Morphological features of doxorubicin-resistant Walker 256 carcinosarcoma and response of mast cells. *Exp. Oncol.* 40:42–47. doi:10.31768/2312-8852.2018.40(1):42-47.
- Bystrom, L. M., and S. Rivella. 2015. Cancer cells with irons in the fire. *Free Radic. Biol. Med.* 79:337–42. doi:10.1016/j.freeradbiomed.2014.04.035.
- Cameron, I. L., M. S. Markov, and W. E. Hardman. 2014. Optimization of a therapeutic electromagnetic field (EMF) to retard breast cancer tumor growth and vascularity. *Cancer Cell Int.* 14:125. doi:10.1186/s12935-014-0125-5.
- Carpenter, D. O. 2010. Electromagnetic fields and cancer: The cost of doing nothing. *Rev. Environ. Health.* 25:75–80. doi:10.1515/reveh.2010.25.1.75.
- Casciato, D. A. 2009. *Manual of clinical oncology*. Philadelphia: Lippincott Williams & Wilkins, Wolters, Kluwer.
- Cichoż-Lach, H., and A. Michalak. 2014. Oxidative stress as a crucial factor in liver diseases. *World J. Gastroenterol.* 20:8082–91. doi:10.3748/wjg.v20.i25.8082.
- Copur, M. S. 2019. State of cancer research around the globe. *Oncology (Williston Park)* 33:181–85.
- Davies, M. J. 2016. Protein oxidation and peroxidation. *Biochem. J.* 473:805–25. doi:10.1042/BJ20151227.
- Deminice, R., S. Padilha Cde, F. Borges, L. E. C. M. Da Silva, F. T. Rosa, J. L. Robinson, R. Cecchini, F. A. Guarnier, F. T. Frajacomo. 2016. Resistance exercise prevents impaired homocysteine metabolism and hepatic redox capacity in Walker-256 tumor-bearing male Wistar rats. *Nutrition* 32:1153–58. doi:10.1016/j.nut.2016.03.008.
- Devrim, E., I. Ergüder, B. Kiliçoğlu, E. Yaykaşı, R. Çetin, İ. Durak. 2008. Effects of electromagnetic radiation use on oxidant/antioxidant status and DNA turn-over enzyme activities in erythrocytes and heart, kidney, liver, and ovary tissues from rats: Possible protective role of vitamin C. *Toxicol. Mech. Methods* 18:679–83. doi:10.1080/15376510701380182.
- Dirican, N., A. Dirican, O. Sen, A. Aynali, S. Atalay, H. A. Bircan, O. Oztürk, S. Erdogan, M. Cakir, A. Akkaya, et al. 2016. Thiol/disulfide homeostasis: A prognostic biomarker for patients with advanced non-small cell lung cancer? *Redox Report* 21:197–203. doi:10.1179/1351000215Y.0000000027.
- Emanuel, N. 1982. *Kinetics of experimental tumor processes*. Oxford: Pergamon Press.
- Faraji, B., H. K. Kang, and J. L. Valentine. 1987. Methods compared for determining glutathione peroxidase activity in blood. *Clin. Chem.* 33:539–43. doi:10.1093/clinchem/33.4.539.
- Ferlay, J., M. Colombet, I. Soerjomataram, C. Mathers, D. M. Parkin, M. Piñeros, A. Znaor, F. Bray. 2019. Estimating the global cancer incidence and mortality in 2018: GLOBOCAN sources and methods. *Int. J. Cancer* 144:1941–53. doi:10.1002/ijc.31937.
- Formelli, F., R. Carsana, and C. Pollini. 1986. Comparative pharmacokinetics and metabolism of doxorubicin and 4-demethoxy-4'-O-methyl-doxorubicin in tumor-bearing mice. *Cancer Chemother. Pharmacol.* 16:15–21. doi:10.1007/BF00255280.
- Gastwirt, J. P., and M. Roschewski. 2018. Management of adults with Burkitt lymphoma. *Clin. Adv. Hematol. Oncol.* 16:812–22.
- Gewirtz, D. A., M. L. Bristol, and J. C. Yalowich. 2010. Toxicity issues in cancer drug development. *Curr. Opin. Investig. Drugs.* 11:612–14.
- Ghodbane, S., M. Ammari, A. Lahbib, M. Sakly, H. Abdelmelek. 2015. Static magnetic field exposure-induced oxidative response and caspase-independent apoptosis in rat liver: Effect of selenium and vitamin E supplementations. *Environ. Sci. Pollut. Res. Int* 22:16060–66. doi:10.1007/s11356-015-4802-2.
- Glazer, E. J., and S. A. Curley. 2011. The ongoing history of thermal therapy for cancer. *Surg. Oncol. Clin. N. Am.* 20:229–35. doi:10.1016/j.soc.2010.11.001.
- Goth, L. 1991. A simple method for determination of serum catalase activity and revision of reference range. *Clinica Chimica Acta* 196:143–51. doi:10.1016/0009-8981(91)90067-m.
- Guillen, J. 2012. FELASA Guidelines and Recommendations. *J. Am. Assoc. Lab. Anim. Sci.* 51:311–21.
- Haanen, J. B. A. G., F. Carbone, C. Robert, K. M. Kerr, S. Peters, J. Larkin, K. Jordan. 2017. Management of toxicities from immunotherapy: ESMO clinical practice guidelines for diagnosis, treatment and follow-up. ESMO guidelines committee. *Ann. Oncol.* 28:119–42. doi:10.1093/annonc/mdx225.
- Hargrove, L., L. Kennedy, J. Demieville, H. Jones, F. Meng, S. DeMorrow, W. Karstens, T. Madeka, J. Greene, H. Francis, et al. 2017. Bile duct ligation-induced biliary hyperplasia, hepatic injury, and fibrosis are reduced in mast cell-deficient Kit W-sh mice. *Hepatology* 65:1991–2004. doi:10.1002/hep.29079.
- Harris, I. S., and G. M. DeNicola. 2020. The complex interplay between antioxidants and ROS in cancer. *Trends Cell Biol.* 30:440–51. doi:10.1016/j.tcb.2020.03.002.
- Harris, I. S., A. E. Treloar, S. Inoue, M. Sasaki, C. Gorrini, K. Lee, K. Yung, D. Brenner, C. Knobbe-Thomsen, M. Cox, et al. 2015. Glutathione and thioredoxin antioxidant pathways synergize to drive cancer initiation and progression. *Cancer Cell* 27:211–22. doi:10.1016/j.ccell.2014.11.019.
- Hawk, M. A., C. McCallister, and Z. T. Schafer. 2016. Antioxidant activity during tumor progression: A necessity for the survival of cancer cells? *Cancers* 8:92. doi:10.3390/cancers8100092.
- Houston, B. J., B. Nixon, B. V. King, G. N. De Iuliis, R. J. Aitken. 2016. The effects of radiofrequency electromagnetic radiation on sperm function. *Reproduction* 152:R263–R276. doi:10.1530/REP-16-0126.
- Jin, Z., C. Zong, B. Jiang, Z. Zhou, J. Tong, Y. Cao. 2012. The effect of combined exposure of 900 MHz radiofrequency fields and doxorubicin in HL-60 cells. *PLoS ONE* 7:e46102. doi:10.1371/journal.pone.0046102.

- Joshi, G., R. Sultana, J. Tangpong, M. P. Cole, D. K. St Clair, M. Vore, S. Estus, D. A. Butterfield. 2005. Free radical mediated oxidative stress and toxic side effects in brain induced by the anti-cancer drug adriamycin: Insight into chemobrain. *Free Radic. Res.* 39:1147–54. doi:10.1080/10715760500143478.
- Jumes, F. M., D. Lugarini, A. L. Pereira, A. de Oliveira, A. D. O. Christoff, G. A. Linde, J. S. do Valle, N. B. Colauto, A. Acco. 2010. Effects of *Agaricus brasiliensis* mushroom in Walker-256 tumor-bearing rats. *Can. J. Physiol. Pharmacol.* 88:21–27. doi:10.1139/Y09-111.
- Kiernan, J. 2008. *Histological and histochemical methods: Theory and practice*. 4th ed. New York: Cold Spring Harbor Laboratory Press.
- Klimanov, M. Y., L. A. Syvak, V. E. Orel, G. V. Lavryk, T. Y. Tarasenko, V. B. Orel, A. Y. Rykhalskiy, V. V. Stegnii, A. O. Nesterenko. 2018. Efficacy of combined regional inductive moderate hyperthermia and chemotherapy in patients with multiple liver metastases from breast cancer. *Technol. Cancer Res. Treat.* 17. doi:10.1177/1533033818806003.
- Kocaman, A., G. Altun, A. A. Kaplan, Ö. G. Deniz, K. K. Yurt, S. Kaplan. 2018. Genotoxic and carcinogenic effects of non-ionizing electromagnetic fields. *Environ. Res* 163:71–79. doi:10.1016/j.envres.2018.01.034.
- Kuzu, M., S. Yildirim, F. M. Kandemir, S. Küçükler, C. Çağlayan, E. Türk, M. B. Dörtbudak. 2019. Protective effect of morin on doxorubicin-induced hepatorenal toxicity in rats. *Chem. Biol. Interact.* 308:89–100. doi:10.1016/j.cbi.2019.05.017.
- Lai, H. 2019. Exposure to static and extremely-low frequency electromagnetic fields and cellular free radicals. *Electromagn. Biol. Med.* 38:231–48. doi:10.1080/15368378.2019.1656645.
- Li, S., H. Y. Tan, N. Wang, Z.-J. Zhang, L. Lao, C.-W. Wong, Y. Feng. 2015. The role of oxidative stress and antioxidants in liver diseases. *Int. J. Mol. Sci.* 16:26087–124. doi:10.3390/ijms161125942.
- Luo, M., L. Shang, M. D. Brooks, E. Jiagge, Y. Zhu, J. M. Buschhaus, S. Conley, M. A. Fath, A. Davis, E. Gheordunescu, et al. 2018. Targeting breast cancer stem cell state equilibrium through modulation of redox signaling. *Cell Metab.* 28:69–86. doi:10.1016/j.cmet.2018.06.006.
- Lushnikova, E. L., E. V. Ovsyanko, L. M. Nepomyashchikh, A. V. Efremov, D. V. Morozov. 2011. Proliferation of Walker 256 carcinosarcoma cells: Effect of whole-body hyperthermia and antitumor agents. *Bull. Exp. Biol. Med.* 152:146–52. doi:10.1007/s10517-011-1475-9.
- Martínez-Sámano, J., P. V. Torres-Durán, M. A. Juárez-Oropeza, D. Elías-Viñas, L. Verdugo-Díaz. 2010. Effects of acute electromagnetic field exposure and movement restraint on antioxidant system in liver, heart, kidney and plasma of Wistar rats: A preliminary report. *Int. J. Radiat. Biol.* 86:1088–94. doi:10.3109/09553002.2010.501841.
- Mattsson, M. O., and M. Simko. 2019. Emerging medical applications based on non-ionizing electromagnetic fields from 0 Hz to 10 THz. *Med. Devices (Auckl)*. 12:347–68. doi:10.2147/MDER.S214152.
- Muramatsu, Y., T. Matsui, M. Deie, K. Sato. 2017. Pulsed electromagnetic field stimulation promotes anti-cell proliferative activity in doxorubicin-treated Mouse Osteosarcoma Cells. *Vivo* 31:61–68. doi:10.21873/invivo.11026.
- Nakata, Y., and A. J. Hopfinger. 1980. An extended conformational analysis of doxorubicin. *FEBS Letter* 117:259–64. doi:10.1016/0014-5793(80)80957-4.
- Naruphontjirakul, P., and K. Viravaidya-Pasuwat. 2019. Development of anti-HER2-targeted doxorubicin-core-shell chitosan nano-particles for the treatment of human breast cancer. *Int. J. Nanomedicine.* 14:4105–21. doi:10.2147/IJN.S198552.
- Odaci, E., D. Ünal, T. Mercantepe, Z. Topal, H. Hancı, S. Türedi, H. Erol, S. Mungan, H. Kaya, S. Çolakoğlu, et al. 2015. Pathological effects of prenatal exposure to a 900 MHz electromagnetic field on the 21-day-old male rat kidney. *Biotech. Histochem* 90:93–101. doi:10.3109/10520295.2014.947322.
- Omote, Y., M. Hosokawa, M. Komatsumoto, T. Namieno, S. Nakajima, Y. Kubo, H. Kobayashi. 1990. Treatment of experimental tumors with a combination of a pulsing magnetic field and an antitumor drug. *Jpn. J. Cancer Res* 81:956–61. doi:10.1111/j.1349-7006.1990.tb02673.x.
- Orel, V., T. Kozarenko, K. Galachin, A. Romanov, A. Morozoff. 2007. Nonlinear analysis of digital images and doppler measurements for trophoblastic tumor. *Nonlinear Dyn. Psychol. Life Sci* 11:309–31.
- Orel, V., A. Shevchenko, A. Romanov, M. Tselepi, T. Mitrelías, C. H. W. Barnes, A. Burlaka, S. Lukin, I. Shchepotin. 2014. Magnetic properties and antitumor effect of nanocomplexes of iron oxide and doxorubicin. *Nanomedicine* 11:47–55. doi:10.1016/j.nano.2014.07.007.
- Orel, V. B., M. A. Zabolotny, and V. E. Orel. 2017. Heterogeneity of hypoxia in solid tumours and mechanochemical reactions with oxygen nanobubbles. *Med. Hypotheses.* 102:82–86. doi:10.1016/j.mehy.2017.03.006.
- Orel, V. E., S. I. Korovin, J. Molnár, V. B. Orel. 2019b. Non-linear dynamics theory and malignant melanoma. *Exp. Oncol.* 41:291–99. doi:10.32471/exp-oncology.2312-8852.vol-41-no-4.13672.
- Orel, V. E., M. Tselepi, T. Mitrelías, A. Rykhalskiy, A. Romanov, V. B. Orel, A. Shevchenko, A. Burlaka, S. Lukin, C. H. W. Barnes. 2018. Nanomagnetic modulation of tumor redox state. *Nanomedicine: Nanotechnology, Biology and Medicine* 14:1249–56. doi:10.1016/j.nano.2018.03.002.
- Orel, V. E., M. Tselepi, T. Mitrelías, M. Zabolotny, M. Krotevich, A. Shevchenko, A. Rykhalskiy, A. Romanov, V. B. Orel, A. Burlaka, et al. 2019a. Nonlinear magnetochemical effects in nanotherapy of Walker-256 carcinosarcoma. *ACS Appl. Bio. Mater* 2:3954–63. doi:10.1021/acsabm.9b00526.
- Ozgun, E., G. Güler, and N. Seyhan. 2010. Mobile phone radiation-induced free radical damage in the liver is inhibited by the anti-oxidants N-acetyl cysteine and epigallocatechin-gallate. *Int. J. Radiat. Biol.* 86:935–45. doi:10.3109/09553002.2010.496029.
- Pliss, E. M., A. M. Grobov, A. K. Kuzaev, A. L. Buchachenko. 2017. Magnetic field effect on the oxidation of hydrocarbons by molecular oxygen. *Mendeleev Commun* 27:246–47. doi:10.1016/j.mencom.2017.05.009.
- Safdie, F., S. Brandhorst, M. Wei, W. Wang, C. Lee, S. Hwang, P. S. Conti, T. C. Chen, V. D. Longo. 2012. Fasting enhances the response of glioma to chemo- and radiotherapy. *PLoS One* 7:e44603. doi:10.1371/journal.pone.0044603.
- Salbitani, G., V. Vona, C. Bottone, M. Petriccione, S. Carfagna. 2015. Sulfur deprivation results in oxidative perturbation in

- Chlorella sorokiniana (211/8k). *Plant Cell Physiol.* 56:897–905. doi:10.1093/pcp/pcv015.
- Sanchez-Valle, V., N. C. Chavez-Tapia, M. Uribe, N. Mendez-Sanchez. 2012. Role of oxidative stress and molecular changes in liver fibrosis. *Curr. Med. Chem.* 19:4850–60. doi:10.2174/092986712803341520.
- Schatten, W. E. 1962. An experimental study of necrosis in tumors. *Cancer Res.* 22:286–90.
- Shaw, R., S. Miller, J. Curwen, M. Dymond. 2017. Design, analysis and reporting of tumor models. *Lab Anim* 46:207–11. doi:10.1038/labani.1257.
- Simkó, M. 2007. Cell type specific redox status is responsible for diverse electromagnetic field effects. *Curr. Med. Chem.* 14:1141–52. doi:10.2174/092986707780362835.
- Tatarov, I., A. Panda, D. Petkov, K. Kolappaswamy, K. Thompson, A. Kavirayani, M. M. Lipsky, E. Elson, C. C. Davis, S. S. Martin, et al. 2011. Effect of magnetic fields on tumor growth and viability. *Comp. Med.* 61:339–45.
- Tayek, J. A., N. W. Istfan, C. T. Jones, K. J. Hamawy, B. R., Bistrián, G. L. Blackburn. 1986. Influence of the Walker 256 carcinosarcoma of muscle, tumor, and whole-body protein synthesis and growth rate in the cancer-bearing rat. *Cancer Res.* 46:5649–54.
- Thoolen, B., R. R. Maronpot, T. Harada, A. Nyska, C. Rousseaux, T. Nolte, D. E. Malarkey, W. Kaufmann, K. Küttler, U. Deschl, et al. 2010. Proliferative and nonproliferative lesions of the rat and mouse hepatobiliary system. *Toxicol Pathol* 38:5S–81S. doi:10.1177/0192623310386499.
- Thorn, C. F., C. Oshiro, S. Marsh, T. Hernandez-Boussard, H. McLeod, T. E. Klein, R. B. Altman. 2011. Doxorubicin pathways: Pharmacodynamics and adverse effects. *Pharmacogenet. Genomics* 21:440–46. doi:10.1097/FPC.0b013e328333ffb56.
- Tipple, T. E., and L. K. Rogers. 2012. Methods for the determination of plasma or tissue glutathione levels. *Methods Mol Biol* 889:315–24. doi:10.1007/978-1-61779-867-2_20.
- Topuz, M., O. Şen, M. Kaplan, O. Akkus, O. Erel, M. Gur. 2017. The role of thiol/disulphide homeostasis in anthracycline as-associated cardiac toxicity. *Int. Heart J* 58:69–72. doi:10.1536/ihj.16-124.
- Tukozkan, N., H. Erdamar, and I. Seven. 2006. Measurement of total malondialdehyde in plasma and tissues by high-performance liquid chromatography and thiobarbituric acid assay. *Firat. Tip. Dergis.* 11:88–92.
- Upshaw, J. N., R. Ruthazer, K. D. Miller, S. K. Parsons, J. K. Erban, A. M. O'Neill, B. Demissei, G. Sledge, L. Wagner, B. Ky, et al. 2019. Personalized decision making in early stage breast cancer: Applying clinical prediction models for anthracycline cardiotoxicity and breast cancer mortality demonstrates substantial heterogeneity of benefit-harm trade-off. *Clin. Breast. Cancer* 19:259–67. doi:10.1016/j.clbc.2019.04.012.
- Usselman, R. J., I. Hill, D. J. Singel, C. F. Martino, et al. 2014. Spin biochemistry modulates reactive oxygen species (ROS) production by radio frequency magnetic fields. *PLoS ONE* 9:e93065. doi:10.1371/journal.pone.0093065.
- Videla, L. A. 2009. Oxidative stress signaling underlying liver disease and hepatoprotective mechanisms. *World J. Hepatol.* 1:72–78. doi:10.4254/wjh.v1.i1.72.
- Walton, E. L. 2016. The dual role of ROS, antioxidants and autophagy in cancer. *Biomed. J.* 39:89–92. doi:10.1016/j.bj.2016.05.001.
- Wieczorek, A., P. M. Stępień, D. Zarębska-Michaluk, W. Kryczka, P. Pabjan, T. Król. 2017. Megamitochondria formation in hepatocytes of patient with chronic hepatitis C - a case report. *Clin. Exp. Hepatol* 3:169–75. doi:10.5114/ceh.2017.68287.
- Wust, P., B. Kortüm, U. Strauss, J. Nadobny, S. Zschaek, M. Beck, U. Stein, P. Ghadjar. 2010. Non-thermal effects of radiofrequency electromagnetic fields. *Sci Rep* 10:13488. doi:10.1038/s41598-020-69561-3.
- Xu, A., Q. Wang, X. Lv, T. Lin. 2021. Progressive study on the non-thermal effects of magnetic field therapy in oncology. *Front. Oncol.* 11:638146. doi:10.3389/fonc.2021.638146.
- Yamashita, N., Y. Kanno, N. Saito, K. Terai, N. Sanada, R. Kizu, N. Hiruta, Y. Park, H. Bujo, K. Nemoto. 2019. Aryl hydro-carbon receptor counteracts pharmacological efficacy of doxorubicin via enhanced AKR1C3 expression in triple negative breast cancer cells. *Biochem. Biophys. Res. Commun.* 516:693–98. doi:10.1016/j.bbrc.2019.06.119.
- Zorov, D. B., M. Juhaszova, and S. J. Sollott. 2014. Mitochondrial reactive oxygen species (ROS) and ROS-induced ROS release. *Physiol. Rev.* 94:909–50. doi:10.1152/physrev.00026.2013.